

# SC-MAS: Constructing Cost-Efficient Multi-Agent Systems with Edge-Level Heterogeneous Collaboration

Di Zhao<sup>1</sup>, Longhui Ma<sup>1</sup>, Siwei Wang<sup>2\*</sup>, Miao Wang<sup>2\*</sup>, Yi Kong<sup>1</sup>

<sup>1</sup>College of Computer Science and Technology, National University of Defense Technology

<sup>2</sup>Academy of Military Sciences

zhaodi@nudt.edu.cn

## Abstract

Large Language Model (LLM)-based Multi-Agent Systems (MAS) enhance complex problem solving through multi-agent collaboration, but often incur substantially higher costs than single-agent systems. Recent MAS routing methods aim to balance performance and overhead by dynamically selecting agent roles and language models. However, these approaches typically rely on a *homogeneous collaboration mode*, where all agents follow the same interaction pattern, limiting collaboration flexibility across different roles. Motivated by *Social Capital Theory*, which emphasizes that different roles benefit from distinct forms of collaboration, we propose **SC-MAS**, a framework for constructing *heterogeneous and cost-efficient* multi-agent systems. **SC-MAS** models MAS as directed graphs, where edges explicitly represent pairwise collaboration strategies, allowing different agent pairs to interact through tailored communication patterns. Given an input query, a unified controller progressively constructs an executable MAS by selecting task-relevant agent roles, assigning edge-level collaboration strategies, and allocating appropriate LLM backbones to individual agents. Experiments on multiple benchmarks demonstrate the effectiveness of **SC-MAS**. In particular, **SC-MAS** improves accuracy by 3.35% on MMLU while reducing inference cost by 15.38%, and achieves a 3.53% accuracy gain with a 12.13% cost reduction on MBPP. These results validate the feasibility of **SC-MAS** and highlight the effectiveness of heterogeneous collaboration in multi-agent systems.

## 1 Introduction

In recent years, Large Language Model (LLM)-based agents have achieved remarkable success across a wide range of tasks, including software development (Hong et al., 2024; Chan et al., 2024; Li et al., 2023), social simulation (Park et al., 2023;

Gao et al., 2023), gaming (Akata et al., 2024; Wang et al., 2023; Tan et al., 2024). Building on the impressive capabilities of single agents, LLM-based Multi-Agent Systems (MAS) have emerged as a powerful paradigm for solving complex problems by leveraging collaboration among agents with specialized roles (Guo et al., 2024; Qian et al., 2024). Meanwhile, the LLM ecosystem has become increasingly diverse, ranging from lightweight and low-cost models to large-scale, high-performance yet expensive alternatives (Matarazzo and Torlone, 2025; Chen et al., 2024b; Ong et al., 2025). This diversity complicates model selection, as larger models do not consistently outperform smaller ones across all tasks and domains (Abdin et al., 2024; Lepagnol et al., 2024; Shen et al., 2024). Consequently, determining how to effectively allocate LLM resources under performance and cost constraints has become a central challenge in practical LLM-based systems.

To address this challenge, prior work (Chen et al., 2024b; Hu et al., 2024) has extensively studied *LLM routing*, which aims to dynamically select appropriate language models for a given input. Early approaches relied on auxiliary encoders such as BERT (Devlin et al., 2019) to decide whether to invoke stronger models (Chen et al., 2024b; Ding et al., 2024; Ong et al., 2025), while more recent methods formulated routing as an optimization problem over performance-cost trade-offs (Feng et al., 2025; Mohammadshahi et al., 2024; Dai et al., 2024). Despite their effectiveness, these approaches primarily focus on single-agent settings and do not consider collaborative interactions among multiple agents. (Chen et al., 2024b; Ong et al., 2025; Feng et al., 2025). In parallel, substantial progress has been made in designing dynamic multi-agent systems (junyou li et al., 2024; Chen et al., 2024a; Wang et al., 2025a). Several studies model MAS as directed acyclic graphs (DAGs) and learn query-specific structures to improve per-

\*Corresponding authors

formance (Zhuge et al., 2024; Wang et al., 2025b; Zhang et al., 2025b). However, these methods typically assume homogeneous agent behaviors or rely on a single LLM backbone, leaving the cost dimension largely unexplored. Conversely, naively applying single-agent LLM routing independently to each agent ignores the rich interaction patterns that emerge from agent collaboration. These limitations highlight the need for a unified framework that jointly considers *which agents to include, how they collaborate, and which LLM resources they should employ*.

Human collaboration provides an important perspective on this problem. According to *Social Capital Theory* (Coleman, 1988; Putnam et al., 2001), effective collective behavior arises not only from individual capabilities but also from the relational ties between individuals. In practice, different pairs of collaborators often adopt distinct interaction patterns, such as critique, debate, depending on their roles and shared objectives. Motivated by this insight, we model a multi-agent system as a structured network, where agents correspond to nodes and edges explicitly encode pairwise collaboration strategies.

Based on this perspective, we propose **SC-MAS**, a Social Capital-driven framework for constructing heterogeneous and cost-efficient Multi-Agent Systems. Given an input query, **SC-MAS** progressively constructs an executable MAS through three stages: (i) selecting task-relevant agent roles from a candidate pool, (ii) establishing edge-level collaboration strategies that explicitly model pairwise interactions between agents, and (iii) assigning appropriate LLM backbones to each agent based on both their roles and collaborative context. These components are jointly optimized to balance task performance and computational cost, enabling flexible and efficient multi-agent collaboration.

Our contributions can be summarized as follows:

- We introduce a social capital-driven perspective on multi-agent system construction, emphasizing the role of relational structures and heterogeneous collaboration strategies in effective MAS design.
- We propose **SC-MAS**, a modular framework that integrates agent selection, collaboration structure construction, and LLM assignment into a unified and efficient system.
- Experiments on five benchmarks show that

**SC-MAS** reduces token consumption by 11.17% to 16.35% while improving accuracy by 1.46% to 3.34% over state-of-the-art methods, validating both its effectiveness and efficiency.

## 2 Related Work

**Dynamic Multi-Agent Systems** Dynamic MAS aim to adapt agent compositions or interaction structures according to task requirements. Existing work has explored search-based methods, such as Monte Carlo Tree Search (Hu et al., 2025; Zhang et al., 2025a; Shang et al., 2025) and evolutionary algorithms (Zhang et al., 2025b), to discover effective agent structures. Recent approaches, including DyLAN (Liu et al., 2024), GPTSwarm (Zhuge et al., 2024), and AgentPrune (Zhang et al., 2025b), model MAS as directed acyclic graphs and optimize collaboration structures in a query-specific manner. However, these methods typically rely on a single LLM backbone and incur substantial computational overhead, limiting their ability to jointly optimize collaboration diversity and cost efficiency in heterogeneous LLM environments.

**Single-Agent LLM Routing** LLM routing has been extensively studied in single-agent settings as a means to balance performance and inference cost. Early work focused on binary routing between small and large models (Chen et al., 2024b; Ding et al., 2024; Ong et al., 2025), while more recent approaches extended routing to multi-model selection and optimization frameworks (Dai et al., 2025; Feng et al., 2025; Chen et al., 2024c). Although effective for single-agent systems, these methods do not account for collaborative interactions among multiple agents and therefore cannot be directly applied to MAS.

**Multi-Agent System Routing** More recently, MasRouter (Yue et al., 2025) introduced MAS routing by jointly determining agent roles, collaboration modes, and LLM allocation. While MasRouter demonstrates strong performance, it adopts a *graph-level* collaboration strategy, where all agents share the same interaction pattern. Such a homogeneous design limits the expressiveness of multi-agent collaboration and fails to capture fine-grained, pairwise interaction patterns that naturally arise in complex tasks. In contrast, our work focuses on *edge-level* collaboration modeling, enabling heterogeneous interaction strategies between different

agent pairs. By explicitly representing collaboration strategies as edges in a graph, **SC-MAS** provides a more expressive and flexible framework for adaptive multi-agent system construction.

### 3 Preliminaries

#### 3.1 MAS as graph with edge strategies

Existing graph-based formulations of MAS (Zhuge et al., 2024; Qian et al., 2025; Wang et al., 2025b) typically represent agents as nodes and communication flows as edges. While effective for information passing, such formulations largely overlook the *collaborative semantics* that govern how agents interact. To explicitly capture heterogeneous collaboration patterns, we model MAS as directed graphs whose edges encode collaboration strategies rather than mere message transmission. Formally, we represent a MAS as a directed acyclic graph  $G = (V, E, L)$ . The graph consists of agent nodes  $V$ , their associated LLMs  $L = \{l_v\}_{v \in V}$ , and directed edges  $E \subseteq V \times V \times S$ . Each edge  $e = (u, v, s) \in E$  denotes agent  $u$  employing strategy  $s \in S$  with respect to agent  $v$ . Strategies are categorized into **edge strategy** ( $S_{edge}$ ,  $u \neq v$ ) and **self-loop strategy** ( $S_{self}$ ,  $u = v$ ) types, allowing representation of both collaboration patterns (e.g. Debate (Liang et al., 2024; Du et al., 2024), Chain (Qian et al., 2025)) and internal reasoning (e.g. Chain-of-Thought (Wei et al., 2022), Reflection (Shinn et al., 2023)). Information is exchanged between the two agents via edge strategy  $s_{eg} \in S_{edge}$ ; in particular, the agent uses self-loop strategy  $s_{sl} \in S_{self}$  each time to give a response.

Given a query  $q$ , the graph  $G$  executes topologically: each agent  $v$  performs its inference process  $f_v$  (using LLM  $l_v$ ) to produce its own output  $o_v = f_v(q, Z_v)$  based on  $q$  and outputs  $Z_v$  from its predecessors. The execution of the graph is described in Algorithm 1.

#### 3.2 Search Space

The search space for MAS configurations is defined over sets of predefined agent roles  $\mathbb{V} = \{v_i\}_{i=1}^{N_V}$ , available LLM backbones  $\mathbb{L} = \{l_i\}_{i=1}^{N_L}$ , edge strategies  $\mathbb{S}_{edge} = \{s_i\}_{i=1}^{N_{eg}}$ , and self-loop strategies  $\mathbb{S}_{self} = \{s_i\}_{i=1}^{N_{sl}}$ . We define the search space components  $(\mathbb{V}, \mathbb{S}_{edge}, \mathbb{S}_{self}, \mathbb{L})$  as  $\mathbb{G}$ .

Constructing an instance  $\mathcal{G} = (\mathcal{V}, \mathcal{E}, \mathcal{L}) \in \mathbb{G}$  requires selecting  $d$  agents  $\mathcal{V} \subseteq \mathbb{V}$ , assigning LLMs  $\mathcal{L} \subseteq \mathbb{L}$ , and choosing an edge set  $\mathcal{E}$ . Potential edges  $(u, v, s)$  connect  $u, v \in \mathcal{V}$  using strategy  $s \in \mathbb{S}_{edge}$

---

#### Algorithm 1 Graph Execution

---

**Require:** MAS graph  $G = (V, E, L)$ , query  $q$ .  
**Ensure:** Final output collection  $O_{final}$ .

- 1: Initialize  $Z \leftarrow$  empty list for each node in the start
- 2: **for** each node  $u$  in  $\text{TopologicalSort}(V)$  **do**
- 3:     Let  $s_{sl}^u$  be the self-loop strategy for  $u$  from  $S_{self}$  (if  $u \rightarrow u$  edge exists, else null)
- 4:     **for** each edge  $(u, v, s_{eg})$  in  $E$  where  $u \neq v$  and source is  $u$  **do**
- 5:         **while** edge strategy  $s_{eg}$  has not been executed **do**
- 6:             Let  $s_{sl}^v$  be the self-loop strategy for  $v$  from  $S_{self}$  (if  $v \rightarrow v$  edge exists, else null)  

▷ agent  $u$  and  $v$  continuously exchange information through the strategy  $s_{eg}$

- 7:              $Z_v \leftarrow Z_v \cup f_u(q, Z_u, s_{sl}^u, s_{eg})$
- 8:              $Z_u \leftarrow Z_u \cup f_v(q, Z_v, s_{sl}^v, s_{eg})$
- 9:         **end while**
- 10:       **end for**
- 11:       **if**  $u$  has no outgoing edges  $(u, v, s_{eg})$  where  $u \neq v$  **then**
- 12:              $O_{final} \leftarrow O_{final} \cup f_u(q, Z_u, s_{sl}^u)$
- 13:       **end if**
- 14: **end for**

---

(for  $u \neq v$ ) or  $s \in \mathbb{S}_{self}$  (for  $u = v$ ). For a chosen  $\mathcal{V}$ , there are  $(N_{sl} \cdot N_{eg}^{d-1})^d$  potential edge sets defined as  $\mathbb{E}$ . A critical constraint mandates that the resulting inter-agent graph structure must be a DAG for valid execution using Algorithm 1. Self-loop strategies, representing local node execution policies, do not affect this topological constraint. The DAG requirement significantly prunes the space of valid edge configurations.

#### 3.3 Query-conditioned MAS Construction

MAS construction is defined as the problem of learning a mapping from an input query  $q$  to an optimal, executable MAS graph  $\mathcal{G} = (\mathcal{V}, \mathcal{E}, \mathcal{L})$ . This mapping is stochastic, represented by a conditional probability distribution  $\mathbb{P}(\mathcal{G} \mid q)$  over valid graphs constructible from the search space components  $(\mathbb{V}, \mathbb{S}_{edge}, \mathbb{S}_{self}, \mathbb{L})$  and satisfying the DAG constraint on inter-agent edges. The mapping is formally defined as:

$$\begin{aligned} f : \mathbb{V} \times \mathbb{S}_{edge} \times \mathbb{S}_{self} \times \mathbb{L} &\rightarrow \mathcal{G}, \\ \pi(\mathcal{G}) &= \mathbb{P}(\{\mathcal{V}, \mathcal{E}, \mathcal{L}\} \mid q) \end{aligned} \quad (1)$$

$$\mathcal{V} \subseteq \mathbb{V}, \mathcal{E} \subseteq \mathbb{E}, \mathcal{L} \subseteq \mathbb{L}, |\mathcal{V}| = |\mathcal{L}|$$

where  $\pi(\mathcal{G})$  represents the probability of selecting  $\mathcal{G}$  under condition query  $q$ .

### 3.4 Optimization Objective

The objective is to learn the conditional distribution  $\mathbb{P}(\mathcal{G} | q)$  that maximizes expected task utility while penalizing execution cost. Given a dataset  $\mathcal{D}$  of query-answer pairs  $(q, a)$ , the optimization problem is formulated as:

$$\max_{\mathbb{P}(\mathcal{G}|q)} \mathbf{E}_{\substack{(q,a) \sim \mathcal{D}, \\ \mathcal{G} \in \mathbb{G} \sim \mathbb{P}(\mathcal{G}|q)}} \left[ \underbrace{U(\mathcal{G}; q, a)}_{\text{Utility}} - \lambda \cdot \underbrace{C(\mathcal{G}; q)}_{\text{Cost}} \right] \quad (2)$$

where  $U(\mathcal{G}; q, a)$  quantifies the utility of the graph  $\mathcal{G}$  (e.g. accuracy evaluated using  $a$ ),  $C(\mathcal{G}; q)$  measures the associated execution cost (e.g., API calls, token usage), and  $\lambda \geq 0$  is a hyperparameter controlling the trade-off between utility and cost.

## 4 SC-MAS

Figure 1 depicts the **SC-MAS** architecture. For an input query  $q$ , **SC-MAS** constructs an executable MAS graph  $\mathcal{G} = (\mathcal{V}, \mathcal{E}, \mathcal{L})$  via three sequential components: Node Selector ( $\mathbb{F}_{\theta_v}$ , Section 4.1), Edge Optimizer ( $\mathbb{F}_{\theta_e}$ , Section 4.2), and LLM router ( $\mathbb{F}_{\theta_l}$ , Section 4.3). The overall generative process for  $\mathcal{G}$  given  $q$  is modeled as  $\mathbb{F}_{\theta}(\mathcal{G} | q)$ , factorized into these components:  $\mathbb{F}_{\theta} = \mathbb{F}_{\theta_v} \circ \mathbb{F}_{\theta_e} \circ \mathbb{F}_{\theta_l}$ . After executing the generated graph  $\mathcal{G}$  to obtain an answer  $a$ , the parameters  $\theta = (\theta_v, \theta_e, \theta_l)$  are updated based on the utility  $U(\mathcal{G}; q, a)$  and cost  $C(\mathcal{G}; q)$  feedback, following the objective in Eq. 2.

This design choice is grounded in a human-centric paradigm informed by *Social Capital Theory* (Coleman, 1988), (Putnam et al., 2001), which posits that cooperative behavior emerges initially at the individual level. According to this theory, individuals form connections and engage in collaboration based on mutual trust and benefit, ultimately leading to the development of structured, goal-oriented networks.

### 4.1 Node Selector

The Node Selector identifies the optimal subset of agents  $\mathcal{V} \subseteq \mathbb{V}$  based on the query  $q$ . Prior work has demonstrated that latent variable-based modeling is effective for adaptive agent selection in dynamic multi-agent systems (Yue et al., 2025), motivating its use in our method. Therefore, in order to model the complex relationship between  $q$  and the potential agents  $v \in \mathbb{V}$ , we employ a variational latent

variable model:

$$\mathbb{F}_{\theta_v}(\mathcal{V} | q) = \int p_v(\mathcal{V} | \mathbf{H}) p_h(\mathbf{H} | q) d\mathbf{H}, \quad (3)$$

$$\mathcal{V} \subseteq \mathbb{V}$$

Here,  $p_h(\mathbf{H} | q) = \mathcal{N}(\mathbf{H}; \mu_t(q), \text{diag}(\sigma_t^2(q)))$  is a Gaussian prior over the latent variable  $\mathbf{H}$ , conditioned on  $q$ . The generator  $p_v(\mathcal{V} | \mathbf{H})$  models the selection of nodes using a factorized Bernoulli distribution:

$$p_v(\mathcal{V} | \mathbf{H}) = \prod_{v \in \mathbb{V}} \pi_v(v | q, \mathbf{H}) \quad (4)$$

$$\pi_v(v | q, \mathbf{H}) \propto \exp(\text{FFN}(f_{\psi}(q) || \tilde{\mathbf{H}}_v) / \tau)$$

$$\tilde{\mathbf{H}}_v = g_{\phi}(f_{\psi}(v), \mathbf{H}), \quad \tau > 0$$

where  $\pi_v$  is the selection probability for node  $v$ , computed using a feed-forward network (FFN).  $f_{\psi}$  is a text encoder (e.g., Sentence-BERT (Reimers and Gurevych, 2019), MiniLM (Wang et al., 2020)) producing embeddings for  $q$  and node descriptions  $v$ .  $g_{\phi}$  is a fusion function generating node-specific contextual representations  $\tilde{\mathbf{H}}_v$  from node embeddings and the latent variable  $\mathbf{H}$ .  $\tau$  is a temperature parameter. Nodes are sampled independently based on  $\pi_v$  to form the set  $\mathcal{V}$  (typically of size  $d$ ).

### 4.2 Edge Optimizer

Given the selected nodes  $\mathcal{V}$ , determined by Section 4.1, the Edge Optimizer determines the set of edges  $\mathcal{E}$ , including both inter-node connections with strategies ( $s_{eg} \in \mathbb{S}_{edge}$ ) and self-loops with internal strategies ( $s_{sl} \in \mathbb{S}_{self}$ ). Unlike previous work (Zhuge et al., 2024), which models edges by assigning a real value representing the likelihood of their existence, our approach extends this representation by assigning a probability distribution to each edge. This distribution captures not only the probability of edge existence but also the likelihood of selecting a particular strategy type. We model the conditional probability distribution  $\mathbb{F}_{\theta_e}(\mathcal{E} | q, \mathcal{V})$  factorized over potential edges:

$$\mathbb{F}_{\theta_e}(\mathcal{E} | q, \mathcal{V}) = \prod_{u, v \in \mathcal{V}, u \neq v} \pi_{eg}((u, v, s_{eg}) | q, u, v, \mathcal{E}_{prev}). \quad (5)$$

$$\prod_{v \in \mathcal{V}} \pi_{sl}((v, v, s_{sl}) | q, v, \mathcal{E}_{prev})$$

where  $\pi_{eg}$  is the probability for inter-node edge  $(u, v, s_{eg})$  and  $\pi_{sl}$  is the probability for self-loop

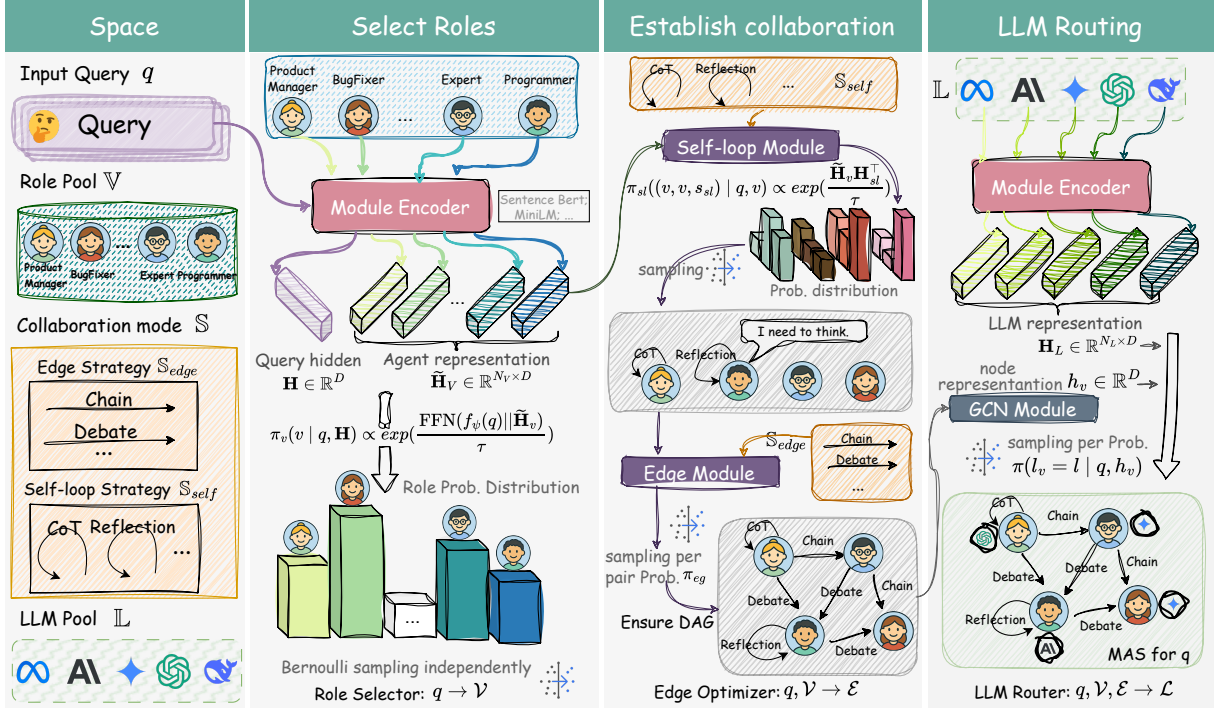


Figure 1: The overall framework of our proposed **SC-MAS**. The roles for accomplishing the query are first selected from the candidate pool, followed by establishing the collaboration relationships between these selected roles, and finally assigning the appropriate LLMs, thus generating an executable graph representation of the heterogeneous collaboration strategies MAS.

$(v, v, s_{sl})$ . These probabilities depend on contextual node representations  $\tilde{\mathbf{H}}_u, \tilde{\mathbf{H}}_v$  (from Eq. 4) and strategy embeddings  $\mathbf{H}_{eg}, \mathbf{H}_{sl}$ :

$$\pi_{eg}((u, v, s_{eg}) | q, u, v, \mathcal{E}_{prev}) \propto \begin{cases} \exp(\tilde{\mathbf{H}}_{u,v} \mathbf{H}_{eg}^T / \tau) & \text{if it's DAG,} \\ 0 & \text{otherwise.} \end{cases} \quad (6)$$

$$\pi_{sl}((v, v, s_{sl}) | q, v, \mathcal{E}_{prev}) \propto \exp(\tilde{\mathbf{H}}_v \mathbf{H}_{sl}^T / \tau)$$

where  $\tilde{\mathbf{H}}_{u,v} = \text{FFN}(\tilde{\mathbf{H}}_u || \tilde{\mathbf{H}}_v)$  denotes the latent representation capturing the implicit relationship between nodes  $u$  and  $v$  under the context of query  $q$ . The terms  $\mathbf{H}_{eg} = \text{FFN}(f_\psi(s_{eg}))$  and  $\mathbf{H}_{sl} = \text{FFN}(f_\psi(s_{sl}))$  represent the hidden embeddings for edge strategies and self-loop strategies, respectively. The crucial DAG constraint ensures that only inter-node edges preserving acyclicity have non-zero probability, effectively pruning cyclic configurations during edge set  $\mathcal{E}$  construction.

### 4.3 LLM Router

Prior studies (Chen et al., 2024b; Ong et al., 2025; Yue et al., 2025) have demonstrated that LLM routing strategies can significantly reduce API costs while maintaining response quality. Finally, the objective of LLM Router is to assign a suitable

LLM  $l \in \mathbb{L}$  to each selected agent  $v \in \mathcal{V}$ , considering the established graph structure  $\mathcal{E}$ . Leveraging the semantic edge strategies, we use a Graph Neural Network (GNN) (Zhou et al., 2020) to capture structural context. An adjacency matrix  $\mathbf{A}$  is constructed where  $\mathbf{A}_{u,v} = f_s(f_\psi(s))$  if  $(u, v, s) \in \mathcal{E}$  (and  $\mathbf{A}_{u,v} = 0$  otherwise), using an edge weighting function  $f_s : \mathbb{R}^D \rightarrow \mathbb{R}$  on strategy embeddings. Applying graph convolution layers:

$$\hat{\mathbf{H}}^{(k)} = \sigma(\tilde{\mathbf{D}}^{-\frac{1}{2}} \tilde{\mathbf{A}} \tilde{\mathbf{D}}^{-\frac{1}{2}} \hat{\mathbf{H}}^{(k-1)} \mathbf{W}^{(k-1)}) \quad (7)$$

where  $\tilde{\mathbf{A}} = \mathbf{A} + \mathbf{I}$ ,  $\tilde{\mathbf{D}} = \text{diag}(\sum_j \tilde{\mathbf{A}}_{i,j})$  is the degree matrix,  $\sigma$  is an activation function,  $\mathbf{W}^{(k)}$  are learnable weights, and initial representations  $\hat{\mathbf{H}}^{(0)}$  are derived from  $\{\tilde{\mathbf{H}}_v \mid v \in \mathcal{V}\}$ . The final GNN node representations  $h_v = \hat{\mathbf{H}}_v^{(K)}$  encode structural and collaborative context. The LLM assignment probability for node  $v$  is then:

$$\begin{aligned} \mathbb{F}_{\theta_l}(\mathcal{L} \mid q, \mathcal{V}, \mathcal{E}) &= \prod_{v \in \mathcal{V}} \pi(l \mid q, h_v) \\ \pi(l \mid q, h_v) &\propto \exp(\text{FFN}(h_v; f_\psi(q))^\top \mathbf{H}_l / \tau), \quad (8) \\ \tau &> 0 \end{aligned}$$

where  $\mathbf{H}_l = \text{FFN}(f_\psi(l))$  is the embedding for candidate LLM  $l$ . This allows assigning LLMs based

Method	LLM backbone	MAS	Routing	MMLU	GSM8K	MATH	HumanEval	MBPP
Vanilla	gpt-4o-mini	✗	✗	77.81	93.17	66.09	85.71	72.20
	claude-3.5-haiku	✗	✗	67.97	92.16	65.89	86.33	73.40
	gemini-1.5-flash	✗	✗	80.04	92.67	74.39	82.61	73.00
	llama-3.1-70b	✗	✗	79.08	92.68	60.31	80.75	68.20
GPTSwarm (Zhuge et al., 2024)	gpt-4o-mini	✓	✗	82.80	94.66	68.85	86.28	75.40
AgentPrune (Zhang et al., 2025b)	gemini-1.5-flash	✓	✗	83.22	93.98	73.35	82.36	74.80
AFlow (Zhang et al., 2025c)	gpt-4o-mini	✓	✗	83.02	94.89	68.45	86.80	75.40
	gemini-1.5-flash	✓	✗	83.10	93.88	73.54	82.55	75.80
PromptLLM (Feng et al., 2025)	gpt-4o-mini	✓	✗	83.10	92.30	73.35	90.06	82.20
	gemini-1.5-flash	✓	✗	82.35	94.91	72.70	85.69	76.00
RouteLLM (Ong et al., 2025)	LLM Pool	✗	✓	78.43	93.92	73.03	86.33	73.60
FrugalGPT (Chen et al., 2024b)	LLM Pool	✗	✓	81.04	93.42	71.29	83.85	72.60
RouterDC (Chen et al., 2024c)	LLM Pool	✗	✓	76.24	90.76	67.05	87.31	74.40
MasRouter (Yue et al., 2025)	LLM Pool	✗	✓	82.01	93.68	73.46	87.75	75.20
SC-MAS (Ours)	LLM Pool	✓	✓	84.25	95.45	75.42	90.62	84.00
	LLM Pool	✓	✓	<b>87.60</b>	<b>96.09</b>	<b>76.75</b>	<b>92.37</b>	<b>87.53</b>

Table 1: Performance comparison across multiple categories of baseline methods, including dynamic multi-agent, single-agent routing and multi-agent routing methods. All models draw from the same candidate LLM pool specified in Section 5.1 to ensure a fair comparison.

on both the node’s role (via  $h_v$ ) and the query context.

#### 4.4 Optimization

The parameters  $\theta$  governing the **SC-MAS** policy  $\mathbb{F}_\theta(\mathcal{G} \mid q)$  are optimized to enhance task performance while considering execution costs. Specifically, we aim to maximize the expected log-likelihood of generating the correct answer  $a$  for a given query  $q$ , penalized by the cost associated with the executed graph  $\mathcal{G}$ . The optimization objective is formulated as:

$$\min_{\theta} \mathbb{E}_{\substack{(q, a) \sim \mathcal{D}, \\ \mathcal{G} \sim \mathbb{F}_\theta}} [-p(a \mid q) + \lambda \cdot C(\mathcal{G}; q)] \quad (9)$$

Here,  $C(\mathcal{G}; q)$  represents the execution cost,  $\lambda \geq 0$  is a hyperparameter balancing performance and cost.  $p(a \mid q)$  is defined as follows:

$$p(a \mid q) = \int_{\mathcal{G} = (\mathcal{V}, \mathcal{E}, \mathcal{L})} \mathcal{O}(a \mid \mathcal{G}) \mathbb{F}_\theta(\mathcal{G} \mid q) d\mathcal{G}, \quad (10)$$

where  $\mathcal{O}(a \mid \mathcal{G})$  denotes the likelihood of obtaining answer  $a$  by executing  $\mathcal{G}$ .  $\mathbb{F}_\theta(\mathcal{G} \mid q)$  was computed in the previous sections. To optimize this objective (Eq. 9), we employ policy gradient (Konda and Tsitsiklis, 1999; Williams, 1992), following common practices in multi-agent structure optimization (Zhuge et al., 2024; Zhang et al., 2025c; Yue et al., 2025). A summary of notations is available in Appendix A, with the detailed algorithm presented in Appendix B.

## 5 Experiments

### 5.1 Experimental Setup

**Datasets** To comprehensively evaluate **SC-MAS** across a diverse set of capabilities, we utilize five widely adopted benchmark datasets: **MMLU** (Hendrycks et al., 2021a), **GSM8K** (Cobbe et al., 2021), **MATH** (Hendrycks et al., 2021b), **HumanEval** (Chen et al., 2021), and **MBPP** (Austin et al., 2021). These datasets collectively encompass a broad range of task domains, including general knowledge, mathematical problem solving, and program synthesis. Following standard practice, we partition each dataset into validation and test subsets using a 1:4 ratio. Specifically for the **MATH** dataset, we adopt the protocol established by prior work (Yue et al., 2025) and perform stratified sampling to construct a subset of 519 problems spanning multiple difficulty levels.

**Baselines** We compare **SC-MAS** against an extensive set of baselines grouped into three categories: (1) dynamic multi-agent systems, such as GPTSwarm (Zhuge et al., 2024), AgentPrune (Zhang et al., 2025b) and AFlow (Zhang et al., 2025c); (2) single-agent LLM routing methods, including PromptLLM (Feng et al., 2025), RouteLLM (Ong et al., 2025), FrugalGPT (Chen et al., 2024b) and RouterDC (Chen et al., 2024c). (3) multi-agent system routing method, represented by MasRouter (Yue et al., 2025).

**LLM Backbones** For consistency and fairness in comparison, we adopt the same set of LLM backbones as used in previous work (Yue et al.,

Dataset	MMLU		GSM8K		MATH		HumanEval		MBPP	
	Acc	Cost (\$)	Acc	Cost (\$)	Acc	Cost (\$)	Acc	Cost (\$)	Acc	Cost (\$)
vanilla SC-MAS	87.60	1.21	96.09	1.33	76.75	3.18	92.37	0.15	87.53	0.91
w/o $\mathbb{F}_{\theta_v}$	85.46	1.29	95.30	1.47	74.37	3.20	87.02	0.16	83.63	0.90
w/o $\mathbb{F}_{\theta_e}$	86.17	1.71	94.92	1.82	73.03	3.71	88.54	0.18	84.50	1.17
w/o $\mathbb{F}_{\theta_l}$	85.96	1.44	94.84	1.44	74.95	3.85	85.50	0.16	85.09	1.29

Table 2: Ablation study of SC-MAS, w/o stands for replacing it with randomized selection.

2025), comprising gpt-4o-mini-0718 (OpenAI, 2024), claude-3.5-haiku (Anthropic, 2024), gemini-1.5-flash (Team et al., 2024), and llama-3.1-70b (Grattafiori et al., 2024). For ablation studies, we additionally include Deepseek-v3 (DeepSeek-AI et al., 2025). The temperature parameters remain at default settings.

**Implementation Details** We adopt all LLMs listed in the LLM Backbones as the candidate model pool for routing methods. To model inter-agent collaboration, we include a diverse edge strategy repository consisting of Chain (Qian et al., 2025), Debate (Chan et al., 2024), and Criticism (Huang and Chang, 2023). For self-loop strategies, we employ CoT (Wei et al., 2022) and Reflection (Shinn et al., 2023). The role pool comprises 26 distinct agent roles, following the configuration proposed by MasRouter (Yue et al., 2025), and spans a wide range of functional expertise across coding, mathematical reasoning, and commonsense domains. We set the learning rate  $\alpha = 0.01$  and the temperature parameter  $\tau = 1$ . We run the experiment three times on each dataset and report the average as the final result. To examine the influence of cost sensitivity in routing decisions, we vary the cost penalty coefficient  $\lambda$  within the set  $\{0, 5, 10, 15, 20\}$ . The report results use  $\lambda$  as 5.

## 5.2 Performance & Cost Analysis

In this section, we compare **SC-MAS** against eight competitive baselines across five representative benchmarks. Our evaluation demonstrates that **SC-MAS** is:

**High Performance.** The experimental results, as detailed in Table 1. Our method achieves SOTA results across all five datasets, including a improvement of 3.35% on the MMLU and 3.53% on MBPP compared to MasRouter. These findings underscore the benefits of incorporating heterogeneous collaboration strategies within MAS, enabling more adaptive and efficient problem solving.

**Inference Token Efficiency.** As illustrated

in Figure 2, **SC-MAS** demonstrates enhanced cost-effectiveness. Compared to MasRouter, our method achieves a 3.53% performance gain while concurrently reducing inference overhead by 12.13% on the MBPP dataset. Similarly, on the HumanEval dataset, it achieves a 1.75% performance gain accompanied by a 16.76% reduction in inference cost. These outcomes underscore the capacity of **SC-MAS** to effectively balance performance with cost.

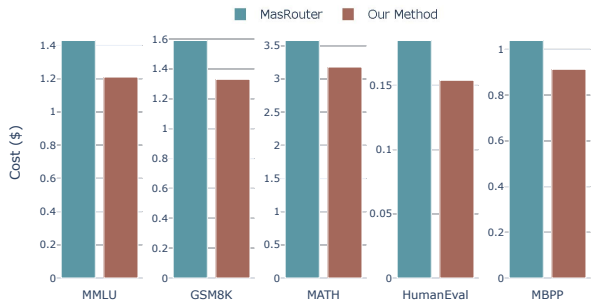


Figure 2: Comparison of inference costs between our work and MasRouter (Yue et al., 2025) across various datasets.

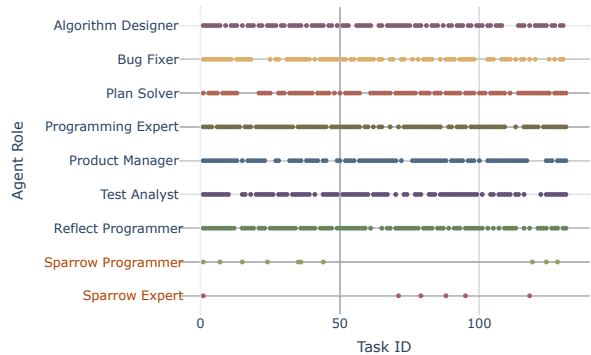


Figure 3: Distribution of roles chosen for reasoning on the HumanEval dataset, with the two roles beginning with Sparrow being the agents coded as error outputs.

## 5.3 Ablation Study

We perform an ablation study to evaluate the contributions of three critical components of **SC-MAS**. The results, summarized in Table 2, highlight the

importance of each module to overall system effectiveness and efficiency. Removing  $\mathbb{F}_{\theta_e}$  resulted in a performance drop of 1.17% to 3.83% and an accompanying cost increase of 16.67% to 41.32%, which underscores the importance of capturing latent relationships among agents for efficient collaboration. Meanwhile, removing  $\mathbb{F}_{\theta_l}$  reduced performance by 1.25% to 6.87% and led to a cost increase of up to 41.76%, indicating that combining diverse LLMs contributes meaningfully to both performance enhancement and cost efficiency.

#### 5.4 Analysis of Unhelpful Agent Filtering

In realistic multi-agent settings, some candidate agents may generate irrelevant or low-quality responses due to role mismatch or limited capability. A practical multi-agent system should be able to reduce the influence of such unhelpful collaborators. To examine this property, we augment the agent pool with two additional roles that deliberately produce random and task-irrelevant outputs. These agents are not designed to perform targeted attacks, but instead act as sources of noisy information. As shown in Figure 3, **SC-MAS** assigns significantly lower selection probabilities to these unhelpful agents (7.63% and 4.58%) compared to task-relevant roles. This suggests that **SC-MAS** can implicitly filter low-quality collaborators during agent selection.

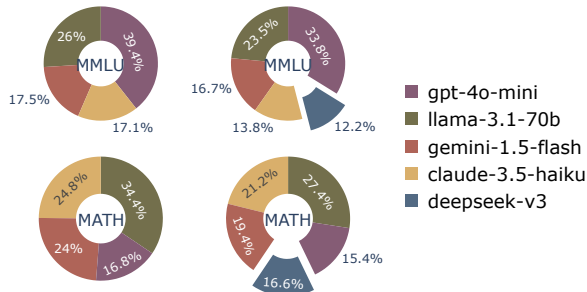


Figure 4: The selected LLM distribution of SC-MAS on MMLU and MATH.

#### 5.5 Inductive Ability Analysis

In this section, we demonstrate that **SC-MAS** can generalize to previously unseen LLMs without re-training. As illustrated in Figure 4, the newly introduced model Deepseek-v3 is selected 12.2% and 16.6% of the time on MMLU and MATH, respectively. After incorporating this stronger LLM, **SC-MAS** achieves increased accuracy on MMLU from 87.60% to 88.14%, and on MATH from 76.75% to 77.84%.

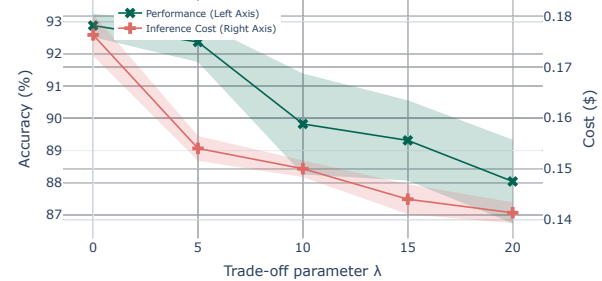


Figure 5: Sensitivity analysis of trade-off parameter  $\lambda$  on HumanEval.

#### 5.6 Sensitivity Analysis

In this section, we perform a sensitivity analysis of the  $\lambda$  parameter introduced in Eq. 9 to balance performance and cost. As  $\lambda$  increases from 0 to 20, the results in Figure 5 illustrate the corresponding trade-offs. When  $\lambda$  is 0, the optimization objective considers only performance, resulting in higher overhead. As  $\lambda$  grows, **SC-MAS** begins to favor more cost-effective solutions, leading to a reduction in overhead by 19.89%, at the expense of a 4.84% performance drop. Thus, adjusting  $\lambda$  according to available resources and task requirements effectively balances performance and cost.

#### 5.7 Case Study

We provide case studies and visualizations of the MAS generated by SC-MAS across five benchmarks in Appendix D.

### 6 Conclusion

In this paper, we study query-conditioned multi-agent system design from a construction perspective and introduce a social capital-driven framework for adaptive and cost-efficient MAS. We propose **SC-MAS**, a high-performance and cost-effective framework for heterogeneous MAS construction. Through its *Node Selector*, *Edge Optimizer*, and *LLM Assigner* modules, **SC-MAS** progressively constructs an executable MAS that balances task performance and computational cost. Our results demonstrate that explicitly modeling edge-level collaboration and resource allocation provides an effective and principled solution for adaptive multi-agent system construction, offering new insights for scalable and flexible LLM-based MAS design.

## 7 Limitation

**Structural Constraints on MAS Topology** To ensure orderly and terminable execution, **SC-MAS** imposes a directed acyclic graph (DAG) structure on the multi-agent system, consistent with prior work. While effective in practice, this constraint inherently limits the expressiveness of the system, precluding cyclical communication patterns and feedback loops that may be beneficial for tasks requiring iterative refinement or mutual verification. This could be a direction for follow-up research.

**Limited Interpretability of Agent and Strategy Selection** Additionally, although **SC-MAS** automatically generates MAS configurations that demonstrate good performance, the rationale behind selecting specific agents, collaboration strategies, and large language models remains non-trivial to interpret. Strengthening the interpretability of MAS generation would enhance user understanding and trust, representing a valuable direction for future research.

## References

Marah Abdin, Jyoti Aneja, Hany Awadalla, and et al. 2024. **Phi-3 technical report: A highly capable language model locally on your phone.** *Preprint*, arXiv:2404.14219.

Elif Akata, Lion Schulz, Julian Coda-Forno, Seong Joon Oh, Matthias Bethge, and Eric Schulz. 2024. **Playing repeated games with large language models.**

Anthropic. 2024. Model card addendum: Claude 3.5 haiku and upgraded claudie 3.5 sonnet. Technical report, Anthropic.

Jacob Austin, Augustus Odena, Maxwell Nye, Maarten Bosma, Henryk Michalewski, David Dohan, Ellen Jiang, Carrie Cai, Michael Terry, Quoc Le, and Charles Sutton. 2021. **Program synthesis with large language models.** *Preprint*, arXiv:2108.07732.

Chi-Min Chan, Weize Chen, Yusheng Su, Jianxuan Yu, and et al. 2024. **Chateval: Towards better LLM-based evaluators through multi-agent debate.** In *The Twelfth International Conference on Learning Representations*.

Lingjiao Chen, Jared Quincy Davis, and et al. 2024a. **Are more LLM calls all you need? towards the scaling properties of compound AI systems.** In *The Thirty-eighth Annual Conference on Neural Information Processing Systems*.

Lingjiao Chen, Matei Zaharia, and James Zou. 2024b. **Frugalgpt: How to use large language models while reducing cost and improving performance.** *Transactions on Machine Learning Research*.

Mark Chen, Jerry Tworek, Heewoo Jun, Qiming Yuan, Henrique Ponde de Oliveira Pinto, and et al. 2021. **Evaluating large language models trained on code.** *Preprint*, arXiv:2107.03374.

Shuhao Chen, Weisen Jiang, Baijiong Lin, James Kwok, and Yu Zhang. 2024c. **RouterDC: Query-based router by dual contrastive learning for assembling large language models.** In *The Thirty-eighth Annual Conference on Neural Information Processing Systems*.

Karl Cobbe, Vineet Kosaraju, Mohammad Bavarian, Mark Chen, Heewoo Jun, Lukasz Kaiser, Matthias Plappert, Jerry Tworek, Jacob Hilton, Reichiro Nakano, Christopher Hesse, and John Schulman. 2021. **Training verifiers to solve math word problems.** *Preprint*, arXiv:2110.14168.

James S Coleman. 1988. Social capital in the creation of human capital. *American journal of sociology*, 94:S95–S120.

Xiangxiang Dai, Jin Li, and et al. 2024. **Cost-effective online multi-llm selection with versatile reward models.** *Preprint*, arXiv:2405.16587.

Xiangxiang Dai, Jin Li, Xutong Liu, Anqi Yu, and John C.S. Lui. 2025. **Cost-effective online multi-LLM selection with versatile reward models.**

DeepSeek-AI, Aixin Liu, Bei Feng, Bing Xue, and et al. 2025. **Deepseek-v3 technical report.** *Preprint*, arXiv:2412.19437.

Jacob Devlin, Ming-Wei Chang, and et al. 2019. **BERT: Pre-training of deep bidirectional transformers for language understanding.** In *Proceedings of the 2019 Conference of the North American Chapter of the Association for Computational Linguistics: Human Language Technologies, Volume 1 (Long and Short Papers)*, pages 4171–4186, Minneapolis, Minnesota. Association for Computational Linguistics.

Dujian Ding, Ankur Mallick, Chi Wang, Robert Sim, Subhabrata Mukherjee, Victor Rühle, Laks V. S. Lakshmanan, and Ahmed Hassan Awadallah. 2024. **Hybrid LLM: Cost-efficient and quality-aware query routing.** In *The Twelfth International Conference on Learning Representations*.

Yilun Du, Shuang Li, Antonio Torralba, Joshua B. Tenenbaum, and Igor Mordatch. 2024. **Improving factuality and reasoning in language models through multiagent debate.** In *Forty-first International Conference on Machine Learning*.

Tao Feng, Yanzhen Shen, and Jiaxuan You. 2025. **Graphrouter: A graph-based router for LLM selections.** In *The Thirteenth International Conference on Learning Representations*.

Chen Gao, Xiaochong Lan, Zhi jie Lu, Jinzhu Mao, and et al. 2023. **S3: Social-network simulation system with large language model-empowered agents.** *ArXiv*, abs/2307.14984.

Aaron Grattafiori, Abhimanyu Dubey, Abhinav Jauhri, Abhinav Pandey, Abhishek Kadian, Ahmad Al-Dahle, Aiesha Letman, Akhil Mathur, Alan Schelten, Alex Vaughan, Amy Yang, Angela Fan, and et al. 2024. **The llama 3 herd of models**. *Preprint*, arXiv:2407.21783.

Taicheng Guo, Xiuying Chen, Yaqi Wang, and et al Chang. 2024. **Large language model based multi-agents: a survey of progress and challenges**. *IJCAI '24*.

Dan Hendrycks, Collin Burns, Steven Basart, Andy Zou, Mantas Mazeika, Dawn Song, and Jacob Steinhardt. 2021a. **Measuring massive multitask language understanding**. In *International Conference on Learning Representations*.

Dan Hendrycks, Collin Burns, Saurav Kadavath, Akul Arora, Steven Basart, Eric Tang, Dawn Song, and Jacob Steinhardt. 2021b. **Measuring mathematical problem solving with the MATH dataset**. In *Thirty-fifth Conference on Neural Information Processing Systems Datasets and Benchmarks Track (Round 2)*.

Sirui Hong, Mingchen Zhuge, Jonathan Chen, Xiaowu Zheng, and et al. 2024. **MetaGPT: Meta programming for a multi-agent collaborative framework**. In *The Twelfth International Conference on Learning Representations*.

Qitian Jason Hu, Jacob Bieker, Xiuyu Li, and et al. 2024. **Routerbench: A benchmark for multi-LLM routing system**. In *Agentic Markets Workshop at ICML 2024*.

Shengran Hu, Cong Lu, and Jeff Clune. 2025. **Automated design of agentic systems**. In *The Thirteenth International Conference on Learning Representations*.

Jie Huang and Kevin Chen-Chuan Chang. 2023. **Towards reasoning in large language models: A survey**. In *Findings of the Association for Computational Linguistics: ACL 2023*, pages 1049–1065, Toronto, Canada. Association for Computational Linguistics.

junyou li, Qin Zhang, Yangbin Yu, QIANG FU, and Deheng Ye. 2024. **More agents is all you need**. *Transactions on Machine Learning Research*.

Vijay Konda and John Tsitsiklis. 1999. **Actor-critic algorithms**. In *Advances in Neural Information Processing Systems*, volume 12. MIT Press.

Pierre Lepagnol, Thomas Gerald, and et al Ghannay. 2024. **Small language models are good too: An empirical study of zero-shot classification**. In *Proceedings of the 2024 Joint International Conference on Computational Linguistics, Language Resources and Evaluation (LREC-COLING 2024)*, pages 14923–14936, Torino, Italia. ELRA and ICCL.

Guohao Li, Hasan Abed Al Kader Hammoud, Hani Itani, Dmitrii Khizbulin, and Bernard Ghanem. 2023. **Camel: communicative agents for "mind" exploration of large language model society**. In *Proceedings of the 37th International Conference on Neural Information Processing Systems*, NIPS '23, Red Hook, NY, USA. Curran Associates Inc.

Tian Liang, Zhiwei He, Wenxiang Jiao, and et al Wang. 2024. **Encouraging divergent thinking in large language models through multi-agent debate**. In *Proceedings of the 2024 Conference on Empirical Methods in Natural Language Processing*, pages 17889–17904, Miami, Florida, USA. Association for Computational Linguistics.

Zijun Liu, Yanzhe Zhang, Peng Li, Yang Liu, and Diyi Yang. 2024. **Dynamic LLM-agent network: An LLM-agent collaboration framework with agent team optimization**.

Andrea Matarazzo and Riccardo Torlone. 2025. **A survey on large language models with some insights on their capabilities and limitations**. *Preprint*, arXiv:2501.04040.

Alireza Mohammadshahi, Arshad Rafiq Shaikh, and Majid Yazdani. 2024. **Routoo: Learning to route to large language models effectively**. *Preprint*, arXiv:2401.13979.

Isaac Ong, Amjad Almahairi, Vincent Wu, Wei-Lin Chang, and et al. 2025. **RouteLLM: Learning to route LLMs from preference data**. In *The Thirteenth International Conference on Learning Representations*.

OpenAI. 2024. **GPT-4o mini: advancing cost-efficient intelligence**. <https://openai.com/index/gpt-4o-mini-advancing-cost-efficient-intelligence/>.

Joon Sung Park, Joseph O'Brien, Carrie Jun Cai, and et al Morris. 2023. **Generative agents: Interactive simulacra of human behavior**. In *Proceedings of the 36th annual acm symposium on user interface software and technology*, pages 1–22.

Robert Putnam and 1 others. 2001. **Social capital: Measurement and consequences**. *Canadian journal of policy research*, 2(1):41–51.

Chen Qian, Wei Liu, Hongzhang Liu, and et al Chen. 2024. **ChatDev: Communicative agents for software development**. pages 15174–15186, Bangkok, Thailand.

Chen Qian, Zihao Xie, YiFei Wang, Wei Liu, Kunlun Zhu, and et al. 2025. **Scaling large language model-based multi-agent collaboration**. In *The Thirteenth International Conference on Learning Representations*.

Nils Reimers and Iryna Gurevych. 2019. **Sentence-BERT: Sentence embeddings using Siamese BERT-networks**. In *Proceedings of the 2019 Conference on Empirical Methods in Natural Language Processing and the 9th International Joint Conference on Natural Language Processing (EMNLP-IJCNLP)*, pages 3982–3992, Hong Kong, China. Association for Computational Linguistics.

Yu Shang, Yu Li, Keyu Zhao, Likai Ma, Jiahe Liu, Fengli Xu, and Yong Li. 2025. **Agentsquare: Automatic LLM agent search in modular design space**. In *The Thirteenth International Conference on Learning Representations*.

Weizhou Shen, Chenliang Li, and et al. 2024. **Small LLMs are weak tool learners: A multi-LLM agent**. In *Proceedings of the 2024 Conference on Empirical Methods in Natural Language Processing*, pages 16658–16680, Miami, Florida, USA. Association for Computational Linguistics.

Noah Shinn, Federico Cassano, Ashwin Gopinath, Karthik Narasimhan, and Shunyu Yao. 2023. **Reflexion: Language agents with verbal reinforcement learning**. *Advances in Neural Information Processing Systems*, 36:8634–8652.

Weihao Tan, Ziluo Ding, Wentao Zhang, Boyu Li, and et al. 2024. **Towards general computer control: A multimodal agent for red dead redemption II as a case study**. In *ICLR 2024 Workshop on Large Language Model (LLM) Agents*.

Gemini Team, Petko Georgiev, Ving Ian Lei, Ryan Burnell, Libin Bai, Anmol Gulati, Garrett Tanzer, Damien Vincent, Zhufeng Pan, Shibo Wang, and et al. 2024. **Gemini 1.5: Unlocking multimodal understanding across millions of tokens of context**. *Preprint*, arXiv:2403.05530.

Guanzhi Wang, Yuqi Xie, Yunfan Jiang, and et al. 2023. **Voyager: An open-ended embodied agent with large language models**. *Trans. Mach. Learn. Res.*, 2024.

Junlin Wang, Jue WANG, Ben Athiwaratkun, Ce Zhang, and James Zou. 2025a. **Mixture-of-agents enhances large language model capabilities**. In *The Thirteenth International Conference on Learning Representations*.

Wenhui Wang, Furu Wei, Li Dong, Hangbo Bao, Nan Yang, and Ming Zhou. 2020. **Minilm: Deep self-attention distillation for task-agnostic compression of pre-trained transformers**. In *Advances in Neural Information Processing Systems*, volume 33, pages 5776–5788. Curran Associates, Inc.

Zhexuan Wang, Yutong Wang, Xuebo Liu, Liang Ding, Miao Zhang, Jie Liu, and Min Zhang. 2025b. **Agentdropout: Dynamic agent elimination for token-efficient and high-performance llm-based multi-agent collaboration**. *Preprint*, arXiv:2503.18891.

Jason Wei, Xuezhi Wang, Dale Schuurmans, Maarten Bosma, and et al Ichter. 2022. **Chain-of-thought prompting elicits reasoning in large language models**. In *Proceedings of the 36th International Conference on Neural Information Processing Systems, NIPS '22*, Red Hook, NY, USA. Curran Associates Inc.

Ronald J Williams. 1992. **Simple statistical gradient-following algorithms for connectionist reinforcement learning**. *Machine learning*, 8(3):229–256.

Yanwei Yue, Guibin Zhang, Boyang Liu, Guancheng Wan, Kun Wang, Dawei Cheng, and Yiyi Qi. 2025. **MasRouter: Learning to route LLMs for multi-agent systems**. In *Proceedings of the 63rd Annual Meeting of the Association for Computational Linguistics (Volume 1: Long Papers)*, pages 15549–15572, Vienna, Austria. Association for Computational Linguistics.

Guibin Zhang, Kaijie Chen, Guancheng Wan, Heng Chang, Hong Cheng, Kun Wang, Shuyue Hu, and Lei Bai. 2025a. **Evoflow: Evolving diverse agentic workflows on the fly**. *Preprint*, arXiv:2502.07373.

Guibin Zhang, Yanwei Yue, and et al. 2025b. **Cut the crap: An economical communication pipeline for LLM-based multi-agent systems**. In *The Thirteenth International Conference on Learning Representations*.

Jiayi Zhang, Jinyu Xiang, Zhaoyang Yu, Fengwei Teng, and et al. 2025c. **AFlow: Automating agentic workflow generation**. In *The Thirteenth International Conference on Learning Representations*.

Jie Zhou, Ganqu Cui, Shengding Hu, Zhengyan Zhang, Cheng Yang, and et al. 2020. **Graph neural networks: A review of methods and applications**. *AI Open*, 1:57–81.

Mingchen Zhuge, Wenyi Wang, Louis Kirsch, and et al Faccio. 2024. **Gptswarm: language agents as optimizable graphs**. In *Proceedings of the 41st International Conference on Machine Learning, ICML'24*. JMLR.org.

## A Notations

For clarity and ease of reference, the commonly used notations throughout the paper are summarized in Table 3.

## B Algorithm Workflow

We conclude the overall algorithm workflow of **SC-MAS** in Algorithm 2

## C Detailed Cost-Performance Data

### C.1 Inference Cost

In this section, we provide a detailed assessment of both the computational overhead and the performance of selected baselines on the MBPP and HumanEval datasets, as summarized in Table 4.

### C.2 Training Cost

We employed an 8G GPU for training, though most of the time was spent waiting for LLM API responses, which depend on the service provider, making direct time comparisons less meaningful. As shown in Table 5, we evaluated the training overhead on the MATH and MMLU datasets in

Notation	Definition
$\mathbb{G} = (\mathbb{V}, \mathbb{S}_{edge}, \mathbb{S}_{self}, \mathbb{L})$	Candidate space containing roles set $\mathbb{V}$ , edge strategies $\mathbb{S}_{edge}$ , self-loop strategies $\mathbb{S}_{self}$ , LLM pool $\mathbb{L}$
$\mathbb{V}$	Set of predefined agent roles (e.g. Analyst, Programmer, Tester)
$\mathbb{S}_{edge}$	Set of inter-agent collaboration strategies (e.g. Debate, Chain)
$\mathbb{S}_{self}$	Set of internal reasoning strategies (e.g. CoT, Reflection)
$\mathbb{L}$	Pool of available LLM backbones
$\mathcal{G} = (\mathcal{V}, \mathcal{E}, \mathcal{L})$	Executable graphical multi-agent system
$\mathcal{V}$	Selected roles set for query $q$
$\mathcal{E}$	Selected edges set for query $q$
$(u, v, s)$	The form of the edge, each $(u, v, s) \in \mathcal{E}$
$\mathcal{L}$	Selected LLM backbone for each agent $v \in \mathcal{V}$
$q$	Input query to multi-agent system
$a$	Oracle answer corresponding to the query $q$
$\mathbb{F}_\theta = \mathbb{F}_{\theta_v} \circ \mathbb{F}_{\theta_e} \circ \mathbb{F}_{\theta_l}$	Controller network for role selector, edge optimizer, and LLM router
$\mathbb{F}_{\theta_v}(\mathcal{V} \mid q)$	Role selector, giving the selected roles $\mathcal{V}$ based on query $q$
$\mathbb{F}_{\theta_e}(\mathcal{E} \mid q, \mathcal{V})$	Edge optimizer, giving the selected edges $\mathcal{E}$ based on query $q$ and selected roles $\mathcal{V}$
$\mathbb{F}_{\theta_l}(\mathcal{L} \mid q, \mathcal{V}, \mathcal{E})$	LLM router, giving the selected edges $\mathcal{L}$ based on query $q$ , selected roles $\mathcal{V}$ , and selected edges $\mathcal{E}$
$\mathbf{H}$	Latent variable capturing query-roles semantics
$\tilde{\mathbf{H}}_v$	Refined representation of the candidate agent role $v$
$p(a \mid q)$	Conditional likelihood of generating answer $a$ via MAS
$C(\mathcal{G}; q)$	Cost function quantifying token expenditure
$\lambda$	Trade-off parameter between utility and cost
$\tau$	Temperature parameter in probability decoding
$f_\psi$	Encoder extracting semantic information from the query $q$
$g_\phi$	Fusion module producing refined representations

Table 3: The notations frequently used throughout this manuscript.

Method	LLM	MBPP		HumanEval	
		Score(%)	Cost(\$)	Score(%)	Cost(\$)
IO	gpt-4o-mini	72.20	0.143	85.71	0.025
	claude-3.5-haiku	73.40	0.146	86.33	0.025
	gemini-1.5-flash	73.00	0.157	82.61	0.032
Complete Graph	llama-3.1-70b	68.20	0.105	80.75	0.013
	gpt-4o-mini	75.20	3.088	85.00	0.488
	gemini-1.5-flash	74.20	1.215	83.75	0.568
LLM Debate	gpt-4o-mini	73.60	4.427	84.38	0.624
	gemini-1.5-flash	73.40	4.529	79.38	0.693
AgentPrune	gpt-4o-mini	75.00	1.215	86.80	0.254
	gemini-1.5-flash	75.60	1.352	82.55	0.271
AFlow	gpt-4o-mini	82.20	1.723	90.15	0.363
	gemini-1.5-flash	76.00	1.832	85.69	0.386
FrugalGPT	llm pool	74.40	0.139	87.31	0.026
RouterDC	llm pool	75.20	0.145	87.75	0.023
MasRouter	llm pool	84.00	1.039	90.52	0.185
SC-MAS	llm pool	87.53	0.913	92.37	0.154

Table 4: Inference Cost-Performance on MBPP and HumanEval Dataset.

---

**Algorithm 2** Workflow of SC-MAS

---

**Input:** Benchmark  $\mathcal{D}$ , encoder  $f_\psi$ , fusion module  $g_\phi$ , learning rate  $\alpha$ , search space  $\mathbb{G} = (\mathbb{V}, \mathbb{S}_{edge}, \mathbb{S}_{self}, \mathbb{L})$

1: **for** query-answer  $(q, a) \in \mathcal{D}$  **do**

2:   **for** iteration  $t \in \{1, 2, \dots, K\}$  **do**

3:     Sample latent vector  $\mathbf{H} \sim \mathcal{N}(\mathbf{H}; \mu_t(q), \text{diag}(\sigma_t^2(q)))$

4:     Compute each agent selected probability:  $\pi_v(v | q, \mathbf{H}) \propto \exp(\text{FFN}(f_\psi(q) || \tilde{\mathbf{H}}_v) / \tau)$

5:     Sampling independently. Selected roles as  $\mathcal{V}$

6:     Let  $\mathcal{E} \leftarrow$  empty set.

7:     **for** each selected node  $u \in \mathcal{V}$  **do**

8:       Compute self-loop strategies probability:  $\pi_{sl}((u, u, s_{sl}))$  ▷ Eq.(6)

9:        $\mathcal{E}$  append  $(u, u, s_{sl})$  if this strategy is sampled

10:      **end for**

11:      **for** each pair  $u, v \in \mathcal{V}$  where  $u \neq v$  **do**

12:       Compute edge strategies probability:  $\pi_{eg}((u, v, s_{eg}))$  ▷ Eq.(6)

13:        $\mathcal{E}$  append  $(u, v, s_{eg})$  if this strategy is sampled

14:      **end for**

15:      Compute the gnn representations  $h_v$  for each  $v \in \mathcal{V}$  ▷ Eq.(7)

16:      Compute LLM compatibility:  $\pi(l_v = l | q, h_v) \propto \exp(\text{FFN}(h_v; f_\psi(q))^\top \mathbf{H}_l / \tau)$

17:      Assign LLM  $l_v$  with multinomial sampling, symbol as  $\mathcal{L}$

18:      Run the MAS  $\mathcal{G} = (\mathcal{V}, \mathcal{E}, \mathcal{L})$  ▷ Algorithm (1)

19:      Compute reward  $R = U(\mathcal{G}; q, a) - \lambda \cdot C(\mathcal{G}, q)$  ▷ Eq.(9)

20:      Update  $\theta$  via policy gradient:  $\theta \leftarrow \theta - \alpha \nabla_\theta \mathbf{E}[-R]$

21:     **end for**

22:   **end for**

---

comparison to other state-of-the-art methods such as GPTSwarm (Zhuge et al., 2024), AFlow (Zhang et al., 2025c), MasRouter (Yue et al., 2025), and our results indicated a substantial reduction in token consumption. Due to our representation of the collaboration strategy as edges, additional time is required to learn the strategy’s relational structures, resulting in higher training overhead than MasRouter. Nevertheless, our completion token usage remains lower than that of MasRouter, highlighting the benefits of a heterogeneous collaboration strategy.

## D Case Study

As shown in Tables 6 to 10, we visualize the customized MAS designed by SC-MAS for varying query difficulties on the five benchmark. In this graph, blue nodes represent the start nodes and orange nodes mark the output nodes; the entire MAS graph is executed according to Algorithm 1, ultimately generating the final output. In this representation of heterogeneous collaboration strategies, two agents automatically establish appropriate collaboration mode based on their relationship with each other.

Method	MATH			MMLU		
	Prompt tokens	Completion tokens	Total cost (\$)	Prompt tokens	Completion tokens	Total cost (\$)
GPTSwarm	23,031,287	6,943,173	7.63	15,525,155	3,983,745	4.70
AFlow	321,813,314	28,083,445	21.75	13,085,019	11,239,502	8.67
MasRouter	3,235,288	2,499,530	3.56	4,459,674	2,904,656	1.43
SC-MAS	17,672,292	1,852,574	5.08	12,808,047	2,083,184	2.64

Table 5: Training Cost comparison between SC-MAS and state-of-the-art baselines on MATH and MMLU.

Query	SC-MAS Workflow
<p>Write a python function to find the minimum number of rotations (greater than 0) required to get the same string.</p> <p>You need to pass these test cases:</p> <pre>assert find_Rotations("aaaa") == 1 assert find_Rotations("ab") == 2 assert find_Rotations("abc") == 3</pre>	
<p>Write a function to flatten a list and sum all of its elements.</p> <p>You need to pass these test cases:</p> <pre>assert recursive_list_sum(     [[1, 2, [3,4],[5,6]])==21 assert recursive_list_sum(     [[7, 10, [15,14],[19,41]])==106 assert recursive_list_sum(     [[10, 20, [30,40],[50,60]])==210</pre>	

Table 6: Case study on MBPP dataset.

Query	SC-MAS Workflow
<p>A fruit vendor bought 50 watermelons for \$80. He sold all of them at a profit of 25%. How much was each watermelon sold?</p>	
<p>A restaurant has 40 tables with 4 legs and 50 tables with 3 legs. Calculate the total number of legs the restaurant's tables have.</p>	

Table 7: Case study on GSM8K dataset.

Query	SC-MAS Workflow
<pre>def is_prime(n):     """Return true if a given number is prime, and false otherwise.      » is_prime(6)     False     » is_prime(101)     True     » is_prime(11)     True     » is_prime(13441)     True     » is_prime(61)     True     » is_prime(4)     False     » is_prime(1)     False     """ </pre>	
<pre>def find_closest_elements(numbers: List[float]) -&gt; Tuple[float, float]:     """ From a supplied list of numbers     (of length at least two) select and return     two that are the closest to each other and     return them in order (smaller number,     larger number).      » find_closest_elements(         [1.0, 2.0, 3.0, 4.0, 5.0, 2.2])     (2.0, 2.2)     » find_closest_elements(         [1.0, 2.0, 3.0, 4.0, 5.0, 2.0])     (2.0, 2.0)     """ </pre>	
<pre>def smallest_change(arr):     """      Given an array arr of integers, find     the minimum number of elements that     need to be changed to make the array     palindromic. A palindromic array is an     array that is read the same backwards     and forwards. In one change, you can     change one element to any other element.      For example:     smallest_change([1,2,3,5,4,7,9,6]) == 4     smallest_change([1, 2, 3, 4, 3, 2, 2]) == 1     smallest_change([1, 2, 3, 2, 1]) == 0     """ </pre>	

Table 8: Case study on HumanEval dataset.

Query	SC-MAS Workflow
What is the positive difference between 120% of 30 and 130% of 20?	
In $\triangle ABC$ , shown, $\cos B = \frac{3}{5}$ . What is $\cos C$ ?  » asy draw((0,0)-(4,0)-(0,3)- cycle,black+linewidth(1)); draw(rightanglemark((4,0),(0,0),(0,3),10), black+linewidth(1)); label("A", (0,0),W); label("B", (0,3),W); label("C", (4,0),E); label("9", (0,0)-(0,3),W); » asy	

Table 9: Case study on MATH dataset.

Query	SC-MAS Workflow
A comet of mass $m$ impacts the earth (mass $M$ radius $R$ ) at the minimum impact speed. What is the expression for the total energy released in the impact?, $m * v, 0.5 * m / (R^3), 0.5 * m * (2GM/R)$ , $0.6 * G(M^2)/R, C$	
Which of the following gives the total spin quantum number of the electrons in the ground state of neutral nitrogen ( $Z = 7$ )?, $1/2, 1, 3/2, 5/2, C$	

Table 10: Case study on MMLU dataset.